RSC Advances

ROYAL SOCIETY OF CHEMISTRY

www.rsc.org/advances

Optical Properties of P and Al doped Silicene : A First Principles Study

Ritwika Das, Suman Chowdhury, Arnab Majumdar[†] and Debnarayan Jana[*]

Here we study the optical properties of two dimensional pure as well as doped buckled silicene nanosheet using density functional theory in the long wavelength limit. Optical properties are studied by varying the concentration of substituted Aluminium (Al), Phosphorus (P) and Aluminium - Phosphorus (Al-P) atoms in silicene nanosheet. It has been observed that unlike graphene, no new electron energy loss spectra (EELS) peak occurs irrespective of doping type for parallel polarization. But for perpendicular polarization two new small yet significant EELS peak emerge for P doping. The origin of these new EELS peak may be explained through the buckling effect of stable silicene. In addition, the calculations have revealed that the maximum values of the absorption coefficient of the doped system are higher than the pristine one. The study on reflectivity modulation with doping concentration has indicated the emergence of some strong peak having robust characteristic of doped reflective surface for both polarizations of electromagnetic field. Moreover, for all doped systems, the reflectivity modulation is restricted to low energy (< 4 eV) and high energy (> 8 eV) for parallel and perpendicular polarization respectively. Although no significant changes are noticed in the maximum values of optical conductivity with doping concentration in perpendicular polarization, however, a sudden jump appears for Al-P codoped system at 18.75% doping concentration. All these theoretical observations are expected to shed light in fabricating opto-electronic devices using silicene as the block material.

1 Introduction

In the world of nanaomaterials having at least one dimension in the nanometre scale and only one dimension is restricted, we get a layered shape or 2D nanomaterials. Naturally, size as well as dimensionality are the two important parameters apart from the material in tailoring the physical properties of materials. Recently, scientists are searching for intriguing 2D layered materials having properties better than graphene[1,2] which could easily be integrated to the current nanoelectronic industry. All these layered structures possess strong in-plane bonding while weak van der Waal (vdW) bonding in a direction perpendicular to the plane[3]. Being a zero band gap material, graphene is not compatible with nano-electronic industry. Beyond graphene, many 2D inorganic materials such as metal oxides, hydroxides etc[4] have been proposed having intriguing physical properties. Out of these, silicene, a two-dimensional buckled honey-comb stable structure has emerged as an alternative to graphene[5]. In contrast to conventional wisdom of absence of crystalline order in two dimension[6], the stability of these two dimensional crystals[7,8] have been argued on the basis of short range structures consisting of the transverse atomic displacements. Besides, the first principles calculations on vibrational properties of silicene have indicated the appearance of characteristic of Raman G-like peak[9] between 570-575 cm^{-1}. In fact, recently theoretical DFT based calculations have pointed out the importance of tip enhanced Raman spectroscopy (TERS) to characterize the buckling distortion in silicene[10]. The electron transport properties of silicene is found to be similar to that of the graphene[11]. Also silicene has an added advantage over graphene that it can be easily interfaced/integrated with the present micro or nanoelectronic devices. It is interesting to note that planar silicene is gapless analogous to zero-mass like Dirac fermions while optimized buckled silicene structure shows a bandgap of 25 meV at K point from local density approximation (LDA) calculations[12]. Moreover, the charge carriers in such a system can move with less scattering. The compatibility of silicene has also been proved both theoretically and experimentally[2,13–15,17–29]. The band structure of silicene is found to be similar to that of the graphene[17]. Although free standing silicene is still difficult to be synthesized till date, however, it has been grown successfully on several metal surfaces such as silver (Ag)[15]. Besides, silicon sheets have been synthesized[16] from chemical exfoliation of hexagonal layered structure calcium disilicide ($CaSi_2$).

The ionic radii of Si is larger than C. So sp^3 hybridization is favourable in silicene than sp^2 hybridization in graphene. As a consequence, a mixing of sp^2 and sp^3 hybridization in silicene[30] results in buckling[17]. The advantage of having buckled structure in silicene is that the band gap can be tuned by applying transverse external static electric field[31–34]. Jose and Datta[35,36] demonstrated the characteristic chemical and structural properties of silicene in compare to graphene. Like B and N doping in graphene[37–41], the natural choice for doping in the

[0]Department of Physics, University of Calcutta, 92 Acharya Prafulla Chandra Road, Kolkata 700009, India

[0†] Present Address: University of Saskatchewan, Saskatoon, Canada S7N 5A1

[0*]*Corresponding Author. E-mail Address: djphy@caluniv.ac.in, Fax: 0091 033 2350 9755*

network of silicene are Aluminium (Al) and Phosphorous (P). It has two major advantages, one is that the atomic radii of Al and P are close to that of Si atom, so the lattice deformation is small due to these kind of doping. Another advantage is, by Al, P codoping substitution, the system remains iso-electronic. Besides, because of the presence of buckling in silicene in contrast to graphene, one may expect higher reactivity towards Al and P. Recently magnetism[42,43] have been demonstrated in silicene under mono-vacancy, di-vacancy, tri-vacancy and substituted atoms such as Al and P. In particular, it has been observed[43] that with a single phosphorus atom as the dopant, the spin polarized magnetism is zero according to local density approximation (LDA) but non-zero ($0.13\mu_B$) in the generalized gradient approximation (GGA) computation of density functional theory (DFT). However, for two P atoms in a hexagonal unit cell, both LDA and GGA give exactly a zero magnetic moment. While for silicene doped with a single Al, a non-zero magnetic moment is obtained both by LDA and GGA. Besides, a significant magnitude of $0.21\mu_B$ is noticed when doped with 2 Al atoms. All these results essentially point out the importance of Al and P doping in the network of silicene. Besides electron energy loss spectroscopy (EELS) and optical absorption being two convenient methods for studying optical properties, EELS study will indicate towards the effective collective mode (plasmon) of excitation of the system. Recently, a prominent change of EELS of multilayer silicene has been observed with the variation of thickness of Ag[44]. In the low energy regime, the EELS spectra have been calculated for free standing α-silicene and β-silicene in the framework of semi-empirical tight binding model[46]. In this calculation[46], the associated peaks in the spectra have been identified with the corresponding electronic transitions between the various k-points in the band structure. Recent calculations on monolayer silicene by Mohan et al[47] have pointed out the anisotropic signature in interband transition in dielectric and EELS study for in plane polarizations and out of plane polarizations. The intriguing relation between the absorption spectra and the dielectric function for free silicene has also been reported in the *ab initio* calculation[45]. First principles calculations on silicene and other group IV honeycomb crystals have indicated[48] that the optical absorption peaks are blue-shifted due to quasi-particle corrections. Also, studying optical properties is very important for designing and characterizing various opto-electronic devices. Motivated by the new structure of silicene and the important results obtained in the study of magnetism for single/double Al and P doping/s in its network, we are interested here to study the optical properties of doped silicene with various doping concentrations of Al (AlS), P (PS) and Al-P (AlPS).

2 Computational details

In this work, all the calculations have been performed within the framework of DFT[49–51], using the GGA according to the Perdew-Burke-Ernzerhof (PBE)[52] parametrization as implemented in SIESTA[53–55] code. Here we have used well tested Troullier - Martin[56], norm conserving pseudopotentials, in fully separable form of Kleinman and Bylander for silicon. The double ζ plus polarized basis set is employed through out the whole range of the systems. The Brillouin zone (BZ) has been sampled by using $20 \times 20 \times 1$ Monkhorst-Pack (MP)[57] of k points. A 300 Ry mesh cutoff has been used for the reciprocal space expansion of the total charge density. The diagonalization method are used to perform all the simulations. For constructing the doped system, the Si atoms of the buckled (0.45 Å) structure is substituted by Al, P and pair of Al-P atoms. In the pristine silicene system three types of substituted atoms concentration have been varied upto 15.62% for AlS and PS system i.e., 5 dopants in 32 atom supercell. For AlPS system, the adatom concentration is varied upto 31.25%, i.e., 5 pairs of of dopant atoms in 32 atom supercell. Throughout the whole calculation we have considered supercell with 32 Si atoms. All these doped structures along with appropriate concentrations are shown in Fig.1. Structures are optimized by minimizing the forces on individual atoms below 0.02 eV/$\AA$ using the standard conjugate-gradient (CG) technique. The convergence criteria for the energy of Self-Consistent Field (SCF) cycle is chosen to be 10^{-4} eV. The typical force convergence of a given structure with 18.75% co-doping with relaxation time steps is shown in Fig.2. The specific doping sites for Al, P and Al-P in the silicene network were chosen by considering the configuration having lowest energy and are consistent with other calculations[58]. All the 2D systems are simulated with 15 $\AA$ of vacuum in the direction perpendicular to the 2D crystal surface in order to avoid the artificial interaction between the artificial images of the 2D sheet. The unit cell of pristine has two Si atoms (A and B) and the space group is P3m1. After the relaxation procedure, the Si - Si, Si - Al and Si - P bond lengths are found to be 2.22, 2.382 and 2.269 $\AA$ respectively. It is interesting to note that the geometry of 2D pristine silicene can be visualized as a bipartite lattice consisting of two interpenetrating triangular sublattices of silicon atoms. However, because π bonds between Si atoms are weaker than that of C atoms, the planarity structure becomes destabilized[59] and as a consequence, two Si planes are buckled with a height of $\Delta = 0.4350\AA$ consistent with the values available in literature ($\Delta = 0.44 - 0.45\AA$) as shown in Fig.3.

The dielectric properties are calculated by using first-order time dependent perturbation theory. In this procedure dipolar transition matrix elements between occupied and unoccupied single electron are computed which is implemented in the SIESTA code within the formalism of Kohn-Sham (KS)[53–55]. To cal-

culate the optical properties, sufficient numbers of unoccupied states above the Fermi level have been used. The self-consistent ground state DFT energies and eigenfunctions have been plugged into the dipolar matrix elements to introduce the exchange and correlation effect. In this way the imaginary part of the dielectric function (ε_2) has been calculated. The real part (ε_1) is calculated with the help of Kramers - Kronig (KK) transformation[60,61]. Optical calculations were done by using $10 \times 10 \times 1$ optical mesh and 0.2 eV optical broadening. For perpendicular polarization, the direction of the electric field is chosen to be incident perpendicular to the plane of the silicene nanosheet, whereas for parallel polarization, it is chosen to be parallel to the plane of the silicene nanosheet.

The modification of the optical properties with respect to three kinds of impurities have been studied. Optical properties of any system[62–64] are in general calculated with the help of frequency dependent complex dielectric function : $\varepsilon(\omega) = \varepsilon_1(\omega) + i\varepsilon_2(\omega)$. The imaginary part is calculated as mentioned earlier with the help of a time dependent perturbation theory in the simple dipole approximation. In the long wavelength limit ($q \to 0$) the imaginary part of the dielectric function[40,53–55,65] is given by,

$$\varepsilon_2(\omega) = \frac{2e^2\pi}{\omega\varepsilon_0} \sum_{K,CB,VB} \left| \left\langle \psi_K^{VB} \middle| \vec{u}.\vec{r} \middle| \psi_K^{CB} \right\rangle \right|^2 \delta(E_K^{CB} - E_K^{VB} - \omega) \tag{1}$$

In the above expression (1), ω is the frequency of the electromagnetic (EM) radiation in energy unit. Ω represents the volume of the supercell and ε_0 is the free space permitivity. CB and VB represent the conduction band and the valence band respectively. $\vec{u}$ and $\vec{r}$ denote the polarization vector and position vector of EM field respectively. The real part and the imaginary part of the complex dielectric functions are connected to each other by KK relation.

For calculating the optical properties, $\varepsilon_2(\omega)$ data is produced by the SIESTA code. Using these set of data, the complex refractive index ($\widetilde{N}$) of any material can be computed by the relation $\widetilde{N} = \sqrt{\varepsilon(\omega)} = n(\omega) + ik(\omega)$,where,

$$n(\omega) = \left(\frac{\sqrt{\varepsilon_1^2 + \varepsilon_2^2} + \varepsilon_1}{2} \right)^{\frac{1}{2}} \tag{2}$$

$$k(\omega) = \left(\frac{\sqrt{\varepsilon_1^2 + \varepsilon_2^2} - \varepsilon_1}{2} \right)^{\frac{1}{2}} \tag{3}$$

The absorption coefficient can be obtained by using the formula,

$$\alpha(\omega) = \frac{2k\omega}{c\hbar} \tag{4}$$

where c represents the speed of light in vacuum and ω is in the energy unit.

The optical conductivity ($\sigma(\omega)$) of any material can be calculated by the relation,

$$\sigma(\omega) = \frac{-i\omega}{4\pi}(\varepsilon(\omega) - 1) \tag{5}$$

The real and the imaginary part of the optical conductivity is respectively given then by,

$$\sigma_1 = \frac{\omega\varepsilon_2}{4\pi} \tag{6}$$

$$\sigma_2 = \frac{\omega}{4\pi}(1 - \varepsilon_1) \tag{7}$$

The direct measure of the collective excitation is the quantity called EELS. It is given by the relation $L(\omega) = Im(-\frac{1}{\varepsilon(\omega)})$ or in terms of ε_1 and ε_2,

$$L(\omega) = \frac{\varepsilon_2}{\varepsilon_1^2 + \varepsilon_2^2} \tag{8}$$

Typical energy of the plasmons of a system can be estimated by looking at the peak positions of any loss function. EELS ($L(\omega)$) attain the maximum value when $\varepsilon_1(\omega) \to 0$ and $\varepsilon_2(\omega) < 1$. All the optical property calculations have been performed in the long wavelength limit $q \to 0$ of EM wave.

3 Results and Discussion

3.1 Formation Energy

Before studying the optical properties of doped silicene, we have studied the defect formation energy of all the structures. The defect formation energy per dopant is defined as

$$E_{df} = \frac{1}{n_{dope}}[E_d + n_{dope}E_{Si} - E_{pris} - n_{dope}E_{dope}]$$

Where n_{dope} is the number of dopants, E_{df}, E_d, E_{Si}, E_{pris} and E_{dope} represent defect formation energy per dopant, total energy of the doped system, energy of a single silicon atom, energy of the pristine silicene system, energy of a single dopant atom respectively. The defect formation energy for Al and P atoms are consistent with recent binding energy calculation from ab-initio calculation for adsorption and absorption silicene[58]. The variation of the defect formation energy per dopant with defect concentration is illustrated in Fig.4. It is seen from the figure, that P doping is more stable than Al and Al-P doping. Also P doping is exothermic in nature, whereas Al doping is found to be endothermic in nature. The higher stability of P atoms in contrast can be routed to the fact that P-Si bond is slightly shorter while Al-Si bond length is larger by $0.1\mathring{A}$ in compared to Si-Si bond length[58]. This slight increase

of Al-Si bond length is due to the lower electronegativity of Al in compared to Si. Besides, it has been argued[58] Al substitution reduces the buckling of silicene while P doping restores its buckling character. In fact, P atoms act as acceptors while Al atoms are donors for silicene. For mixed doping, it is observed that the process is exothermic but at 18.75% co-doping concentration, it suddenly becomes endothermic.

3.2 Dielectric function

Different optical properties of pristine silicene is depicted in Fig 5. Fig 5(a) and Fig 5(b) respectively depicted the real and imaginary part of the dielectric function of pristine silicene with both parallel ($E_{||}$) and perpendicular ($E_{\perp}$) polarization of the electric field vector of the external EM field in long wavelength limit ($q \to 0$). The static value of the real part of the dielectric function ($\varepsilon_1(0)$) for pristine silicene is respectively given as 5.41 and 1.64 for $E_{||}$ and $E_{\perp}$. The structure peaks in ε_2 related to inter-band transitions as observed in Fig 5(b) for parallel ($E_{||}$) and perpendicular ($E_{\perp}$) polarization are situated at 1.01 eV, 3.91 eV, 5.16 eV and 6.18 eV, 8.86 eV respectively. Some of these peaks (3.91 eV and 8.86 eV) are in agreement with the observation in LDA based calculations[47]. Besides, the peaks below 3 eV are known[47] to be connected with $\pi - \pi^*$ transitions along the M-K while those above 3 eV with $\sigma - \sigma^*$ along the M-K and $\Gamma - K$ directions. The variation of $\varepsilon_1(0)$ with Al, P and Al-P doping concentration is depicted in Fig 6. In case of $E_{\perp}$, for both AlS and PS system, we can observe an overall increasing tendency, but for AlPS system, we can see an overall constant behavior. For $E_{||}$, in case of AlS system , the parabolic shape of the graph is observed. For PS system, after slight increase, again it starts decreasing and reaches the minima at 12.50% of doping then again it starts increasing. It would be interesting to see the behavior for still higher P doping concentration. For AlPS system of doping, a zigzag behavior is observed with maximum value at 18.75% co-doping.

3.3 Electron energy loss spectra (EELS)

Electron energy loss spectroscopy (EELS) of pristine silicene is depicted in Fig 5(d). From the figure it is evident that pristine silicene has two plasmon peaks in parallel polarization, one is around 2 eV which is due to π plasmon and the other is around 9 eV which is due to $\pi + \sigma$ plasmon. In particular, the peak at 2 eV is caused by the transition between π and π^* bands around M and Γ point in the band structure. However, other peak at 9 eV can be ascribed to the transition between the 4th valence band and the π^* conduction band. The peak at 11 eV in perpendicular polarization for pristine silicene can be identified with third valence band and conduction band in α silicene. These observations are consistent with the tight-binding calculation of the band structure and the calculation of dielectric function in the random phase approximation for β silicene[45,46] and LDA based calculations[47]. For Al and P doped systems, inspite of the presence of some additional peaks in the EELS spectra, It has been observed (not shown in figure) the major peaks in parallel polarizations are red-shifted while for perpendicular polarizations, they are blue-shifted compared to pristine silicene. However, with increase of doping concentration, all the peaks are red-shifted irrespective of the nature of polarizations. The blue-shifting of the peaks in perpendicular polarization is due to the bucking introduced in the silicene nanosheet.

The variation of EELS peak in perpendicular polarization for various doping concentration of Al, P and Al-P co-doped systems are presented in Fig.7. Fig 7(top panel left) illustrates the EELS spectra for various P doping concentrations for $E_{\perp}$. It is to be noted from the figure that two new small peaks appear near 8 eV and 9.5 eV apart from the large peak around 11 eV. The origin of these two small peaks is possibly due to out of plane plasmon excitation. For parallel polarization, in Al-P co-doped system, the 2 eV peak in pristine silicene at 6.25% shifted to 2.22 eV. With further increase of doping concentration, it is shifted to low energy regime. One of the major peak around 8 eV is shown in Fig 7 for various doping concentration of Al-P. However, for perpendicular polarization apart from the strong peaks around 11 eV and 8 eV, the two small new peaks emerge around 9.78 eV at 6.35% and 12.5%. It is interesting to note that unlike graphene, silicene possesses a small buckling due to Jahn-Teller distortion. Due to this buckling[17] it is natural to expect the out of plane plasmon excitations in silicene and rich complex structure in EELS as noted recently in case of pristine silicene[46]. We summarize the variation of the maximum EELS peak nature with doping concentration of Al, P and Al-P co-doping in Fig.7(bottom panel right). In particular, we schematically plot the frequencies at which EELS attain maximum values with increasing doping concentration. From the figure it is evident that in case of $E_{\perp}$ for all three types of doping, an overall decreasing tendency in frequency is observed. But for $E_{||}$, for AlS and PS system, initially it gets slightly increased but then again starts decreasing upto 12.50 % of doping. After that it again starts increasing. Again it would be interesting in future to see the frequency shift for still higher Al and P doping concentration. For AlS and PS system again a zigzag behavior is observed like previous case.

3.4 Optical absorption

Absorption coefficient ($\alpha(\omega)$) of pristine silicene is depicted in Fig 5(c). The maximum value of the absorption coefficient for pristine silicene is 13.55 at energy 4.07 eV for $E_{||}$ which is within the ultraviolet range and 16.35 at energy 9.11 eV for $E_{\perp}$ which is also in the ultraviolet energy range. But for doped system the value of absorption coefficient is higher than the pristine silicene. For parallel polarization, the maximum ab-

sorption coefficients are blue-shifted in compared to the pristine system irrespective of doping concentration. While for perpendicular polarization it is interesting to note that for PS and AlPS system we observe a red-shift of the maximum absorption coefficients. For AlS system depending upon the concentration there are both blue as well as red shift of the maximum value of the absorption coefficients. Fig 8 illustrates the variation of $\alpha_{max}(\omega)$ with doping concentration. For $E_{\perp}$, irrespective of type of doping, all show a decreasing tendency towards high doping concentration. For PS system, the maximum value of $\alpha(\omega)$ is noticed to be within the frequency range of 8-9 eV irrespective of doping concentration. Similarly for AlS system this value is around 9-10 eV. For AlPS doping this value lies within 9 eV. In case of $E_{||}$, this value is around 4.5 eV, 5 eV and 5-9 eV for PS, AlS and AlPS system respectively. Irrespective of doping and polarization, beyond the frequency range of around 15 eV, very low value of absorption coefficient is observed.

3.5 Optical conductivity

The real ($\sigma_1(\omega)$) and imaginary ($\sigma_2(\omega)$) part of the frequency dependent optical conductivity of the pristine silicene is depicted in Fig 5(e) and Fig 3(f) respectively. In case of pristine silicene the maximum value of the real part is noticed around 4 eV and around 9 eV for $E_{||}$ and $E_{\perp}$ respectively. The maximum value of $\sigma_1(\omega)$ for various doping concentrations is illustrated in Fig 9. For $E_{\perp}$, more or less constant behavior is observed for both AlS and PS system. Whereas for AlPS system, a sudden jump in the conductivity is observed for 18.75% doping concentration. For $E_{||}$, characteristic feature is noticed for different types of doping. For PS system, zigzag behavior is observed, for AlS system, an increasing tendency is seen and for AlPS system an overall increasing behavior is obtained. So it can be concluded that the optical conductivity of silicene can be controlled by appropriate doping with Al, P or both Al-P. It is worthy to note that the variation of $\sigma_1(\omega)$ is consistent with that of the imaginary part of the dielectric function. This naturally serves as a cross-check to our numerical computation. This can shed light for the possible use of silicene in opto-electronic devices.

3.6 Reflectivity Modulation

To analyze the spectra of reflectivity, it is desirable to concentrate on the reflectivity (R) modulation with energy (ω) given by,

$$R_M(\omega) = \frac{1}{R(\omega)} \frac{dR(\omega)}{d\omega}$$

In fact, reflectivity modulation is a convenient way to analyze the characteristic feature of reflectivity spectrum of any material[66]. It is interesting to note that although $R(\omega)$ by its very definition is always positive, however, $R_M(\omega)$ can be of any sign. The modulation data for all the doped systems with energy for both type of polarizations are depicted in Fig 10. The anisotropic features associated with two polarizations are quite evident from the figure. In particular, for all doped systems, the reflectivity modulation is restricted within low energy (< 4 eV) and high energy (> 8 eV) for $E_{||}$ and $E_{\perp}$ respectively. For AlS in $E_{||}$, the peak below 1 eV with increase of doping concentration shifts slightly towards higher energy with varying amplitudes. The same signature continues to exist even for peak near 2 eV. However, the peak at 8 eV in $E_{\perp}$ remains robust in its energy position with small variation of its amplitudes. In $E_{||}$ of PS system, for three different concentration 3.12%, 6.24% and 9.37% the peak near 2 eV shifts slightly to higher energy and this peak vanishes away with higher concentration of P. However, the prominent peak near 8 eV in $E_{\perp}$ sustains its feature till 9.37%. The other significant peak at 10 eV in this system is noticed to change its amplitude very small keeping its position fixed with increase of doping concentration of P. This peak can be identified as one of the characteristic signals of any PS system. For AlPS systems, the existence of two significant peaks at 8 and 10 eV in $E_{\perp}$ is important for all concentrations. The presence of multiple peaks in $E_{\perp}$ at high energy and $E_{||}$ at low energy is again an indication of buckling in the silicene system.

4 Conclusions

In summary, the optical properties of free standing silicene with various concentration of Al, P and Al-P codoping have been performed in the framework of DFT in the long wavelength limit. It is demonstrated from the formation energy that structures with P doping are more stable compared with other doped ones. With increase of doping concentration, the peaks in EELS spectra are red-shifted irrespective of the nature of polarization. At some particular P doping concentration, new additional significant EELS peak is observed in perpendicular polarization. It is also noted that for doped system the value of absorption coefficient is higher than the pristine silicene and is restricted within the ultraviolet range. Although no significant changes are indicated at the maximum values of optical conductivity with doping concentration in perpendicular polarization, however, a sudden jump appears for Al-P codoped system at 18.75% doping concentration. Besides for all doped systems, the reflectivity modulation is restricted within low energy (< 4 eV) and high energy (> 8 eV) for $E_{||}$ and $E_{\perp}$ respectively. The presence of multiple peaks in the modulation can be related to the buckling of the silicene. Although the above theoretical results are obtained with GGA and 32 atoms, however, we believe that these predicted results may give a strong indication in experimental situation with Al and P doped silicene systems. All these theoretical observations are expected to shed light in fabricating opto-electronics devices using silicene as the block material.

5 Acknowledgements

This work is partially supported by DST-FIST, DST-PURSE, Government of India. Two of the authors (RD and SC) gratefully acknowledge DST, Government of India for providing financial assistance through DST-INSPIRE Fellowship scheme. The authors would also like to take this opportunity to thank two anonymous reviewers for their critical comments and suggestions.

References

[1] A. K. Geim and I. V. Grigoriera, Nature, **499**, 419 (2013).

[2] M. Xu, T. Liang, M. Shi, H. Chen, Chem. Rev., 2013, **113**, 3766.

[3] V. Nicolosi, M. Chhowala et al., Science 2013, **340**, 1226419.

[4] R. M.-Balleste, C. G.-Navarro et al., Nanoscale 2011, **3**, 20.

[5] L. C. L. Y. Voon and G. G. G-Veri, MRS Bulletin 2014, **39**, 366. See also, G. G. G-Veri and L. C. L. Y. Voon, Phys. Rev B 2007, **76**, 75131.

[6] N. D. Mermin, Phys. Rev 1968, **176**, 250.

[7] H.O'Hare, F. V. Kusumartsov and K. I. Kugel, Nano Lett 2012, **12**, 1045.

[8] N. J. Roome and J. D. Caret, ACS Appl. Mater. Interfaces 2014, **6**, 7743.

[9] E. Scalise, M. Houssa, G. Pourtois et al, Nano Res. 2013, **6**, 19.

[10] D. Jose, A. Nijamudheen and A. Datta, Phys Chem Chem Phys 2013, **15**, 8700.

[11] W. -F. Tsai, C. -Y. Huang, T. -R. Chang, H. Lin, H. -T Jeng, and A. Bansil, Nat Commun, 2013, **4**, 1500.

[12] H. Behera and G. Mukhopadhyay, " A Comparative computational study of the electronic properties of planar and buckled silicene", arXiv:1201.1164.

[13] A. Kara, et. al, J. Supercon. Nov. Magn., 2009, **22**, 259.

[14] B. Aufray, et. al, Appl. Phys. Lett., 2010, **96** 183102.

[15] D. E. Padova, C. Quaresima, et. al., Appl. Phys. Lett., 2011, **98**, 081909.

[16] H. Nakano, T. Mitsuoka et. al., Angew Chem. 2006, **118**, 6451.

[17] S. Lebgue, O. Eriksson, Phys. Rev. B, 2009, **79**, 115409.

[18] H. Sahin, S. Cahangirov, M. Topsakal, E. Bekaroglu, E. Aktrk, R. T. Senger, S. Ciraci, Phys. Rev. B, 2009, **80**, 155453.

[19] S. Cahangirov, M. Topsakal, E. Aktrk, H. Sahin, S. Ciraci, Phys. Rev. Lett., 2009, **102**, 236804.

[20] S. Wang, J. Phys. Soc. of Jpn., 2010, **79**, 064602.

[21] M. Houssa, G. Pourtois, V. V. Afanasev, A. Stesmans, Appl. Phys. Lett., 2010, **97**, 112106 .

[22] B. Lalmi, H. Oughaddou, H. Enriquez, A. Kara, S. Vizzini, B. Ealet and B. Aufray, Appl. Phys. Lett., 2010, **97**, 223109.

[23] P. Vogt, P. D. Padova, C. Quaresima, J. Avila, E. Frantzeskakis, M. C. Asensio, A. Resta, B. Ealet, G. L. Lay, Phys. Rev. Lett., 2012, **108** 155501.

[24] N. Y. Dzade, K. O. Obodo, S. K. Adjokatse, A. C. Ashu, E. Amankwah, C. D. Atiso, A. A. Bello, E. Igumbor, S. B. Nzabarinda, J. T. Obodo, A. O. Ogbuu, O. E. Femi, J. O. Udeigwe, U. V. Waghmare, J. Phys. : Condens. Matter, 2010, **22**, 375502.

[25] D. Jose, A. Datta, Phys. Chem. Chem. Phys., 2011, **13**, 7304.

[26] M. J. S. Spencer, T. Morishita, M. Mikami, I. K. Snook, Y. Sugiyama, H. Nakano, Phys. Chem. Chem. Phys., 2011, **13**, 15418.

[27] T. H. Osborn, A. A. Farajian, O. V. Pupysheva, R. S. Aga, L. C. L.Y. Voon, Chem. Phys. Lett., 2011, **511**, 101.

[28] P. D. Padova, C. Quaresima, C. Ottaviani, P. M. Sheverdyaeva, P. Moras, C. Carbone, D. Topwal, B. Olivieri, A. Kara, H. Oughaddou, B. Aufray, G. L. Lay, Appl. Phys. Lett., 2010, **96**, 261905.

[29] A. Kara, H. Lneiquez, A. P. Seitsonen et al, Surf. Science. Rep., 2012, **67**, 1.

[30] E. Cinquanta, E. Scalise, D. Chiappe et al., J. Phys. Chem. C, **117**, 16719 (2013).

[31] C. Kamal, http://arxiv.org/abs/1202.2636 . See also, C. Kamal, A. Chakrabarti, A. Banerjee and S. K. Deb, J. Phys.: Cond. Matter 2013, **25**, 085508.

[32] Z. Ni, Q. Liu, K. Tang, J. Zheng, J. Zhou, R. Qin, Z. Gao, D. Yu, J. Lu, Nano Lett., 2012, **12**, 113.

[33] N. D. Drummond, V. Z lyomi, V. I. Falko, Phys. Rev. B, 2012, **85**, 075423.

[34] M. Ezawa, New Journal of Physics, 2012, **14**, 033003.

[35] D. Jose, A. Datta, J. Phys. Chem C, 2012, **116**, 24639.

[36] D. Jose, A. Datta, Acc. Chem. Res., 2014, **47**, 593.

[37] P. Nath, D. Sanyal, D. Jana, Physica E, 2014, **56**, 64.

[38] P. Rani and V. K. Jindal, RSC Advances, 2013, **3**, 802.

[39] P. Rani and V. K. Jindal, "Stability and electronic properties of isomers of B/N co-doped graphene", Appl Nanosci, 2013, doi: 10.1007/s13204-013-0280-3

[40] P. Nath, S. Chowdhury, D. Sanyal and D. Jana, Carbon, 2014, **73**, 275.

[41] D. Jana, P. Nath and D. Sanyal, "Modifications of Electronic properties of Graphene by Boron (B) and Nitrogen (N) substitution", To appear as a chapter in CRC Press/Taylor & Francis, 2014.

[42] V. O. *Ö*zcelik and S. Ciraci, Phys. Rev. B, 2012, **86**, 155421

[43] A. Majumdar, S. Chowdhury, P. Nath and D. Jana, RSC Advances, 2014, **4**, 32221

[44] L. Rast, and V. K. Tewary, Electron Energy Loss Function of Silicene and Germanene Multilayers on Silver, 2013, arxiv: 1311:0838v1.

[45] K. Chinnathambi, A. Chakrabarti, A. Banerjee, S.K. Deb, Optical Properties of Graphene-like Two Dimensional Silicene, arXiv:1205.5099 [cond-mat.mes-hall] (2012)

[46] Luis M. Priede and Lilia Meza-Montes, Electron-Energy-Loss Spectra of Free-Standing Silicene, arXiv:1405.4205 [cond-mat.mes-hall] (2014).

[47] B. Mohan, A. Kumar and P. K. Ahluwalia, Physica E 2013, **53**, 233. .

[48] L. Matthes, O. Pulici and F. Bechstedt, J. Phys.: Condens. Matter, 2013, **25**, 395305.

[49] P. Hohenberg, W. Kohn, Phys. Rev., 1964, **136** B864.

[50] W. Kohn, L. J. Sham, Phys. Rev., 1965, **140**, A1133.

[51] W. Kohn, Rev. Mod. Phys., 1999, **71**, 1253.

[52] J. P. Perdew, K. Burke, M. Ernzerhof, Phys. Rev. Lett., 1996, **77**, 3865.

[53] P. Ordejon, E. Artacho, J. M. Soler, Phys. Rev. B, 1996, **53**, R10441.

[54] D. Sanchez-Portal, P. Ordejon, E. Artacho, J. M. Soler, Int. J. Quantum Chem., 1997, **65**, 453.

[55] J. M. Soler, E. Artacho, J. D. Gale, A. Garca, J. Junquera, P. Ordejon, D. Sanchez-Portal, J. Phys. : Condens. Matter., 2002, **14**, 2745 ; see also http://www.uam.es/siesta.

[56] N. Troullier, J. L. Martins, Phys. Rev. B, 1991, **43**, 1993.

[57] H. J. Monkhorst, J. D. Pack, Phys. Rev. B, 1976, **13**, 5188.

[58] J. Sivek, H. Sahin et al, Phys. Rev. B, 2013, **87**, 085444.

[59] H-X. Luan, C-W. Zhang, F-B. Zheng and P. Wang, J. Phys. Chem C 2013, **117**, 13620.

[60] G. D. Mahan, Many Particle Physics. New York: Plenum Press; 1990.

[61] M. Dressel, G. Gruner, Electrodynamics of Solids. Cambridge: Cambridge University Press; (2002)

[62] D. Jana, L. -C. Chen, C. W. Chen, S. Chattopadhyay, K. H. Chen, Carbon, 2007, **45**, 1482.

[63] D. Jana, A. Chakraborty, L. -C. Chen, C. W. Chen, K. H. Chen, Nanotechnology, 2009, **20**, 175701.

[64] S. Chowdhury, Ritwika Das, P. Nath, D. Sanyal and D. Jana, "Electronic and Optical properties of Boron and Nitrogen functionalized graphene nanosheet" (Accepted by CRC Publications, Taylor & Francis, 2014).

[65] D. Jana, C. L. Sun, L. -C. Chen, C. H. Chen, Prog. Mater. Sci., 2013, **58**, 565.

[66] P. Y. Yu, M. Cardona, "Fundamentals of Semiconductors Physics and Materials Properties", 4 ed. Springer Publication, Chapter 6.

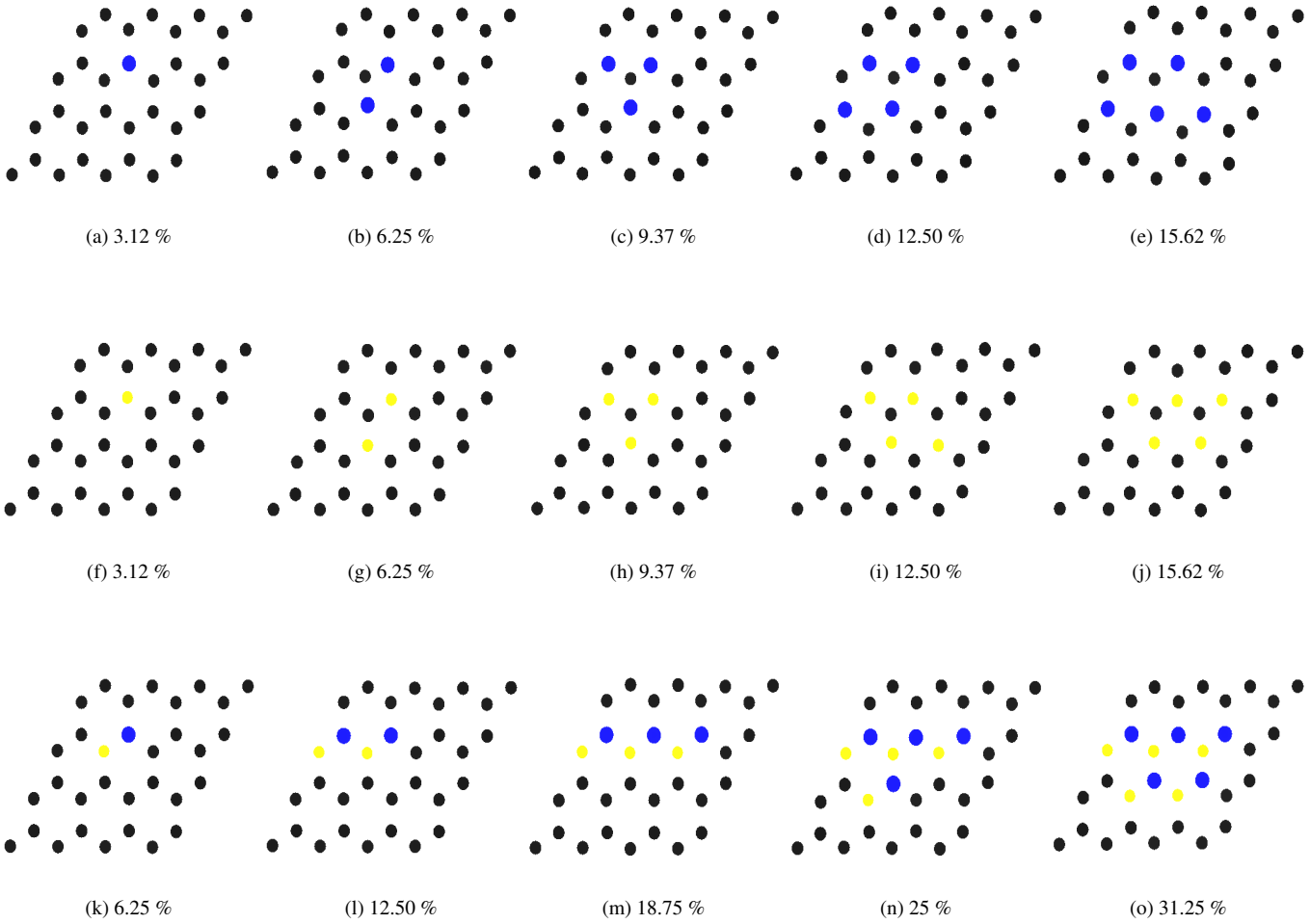

(a) 3.12 % (b) 6.25 % (c) 9.37 % (d) 12.50 % (e) 15.62 %

(f) 3.12 % (g) 6.25 % (h) 9.37 % (i) 12.50 % (j) 15.62 %

(k) 6.25 % (l) 12.50 % (m) 18.75 % (n) 25 % (o) 31.25 %

Fig. 1: Different structures of doped 32 atom Silicene supercell. Black, blue and yellow balls respectively indicate Si, Al and P atom. (Top) (a) - (e) Different structures of Al doped Silicene. (Middle) (f) - (j) Different structures of P doped Silicene. (Bottom) (k) - (o) Different structures of Al - P doped Silicene

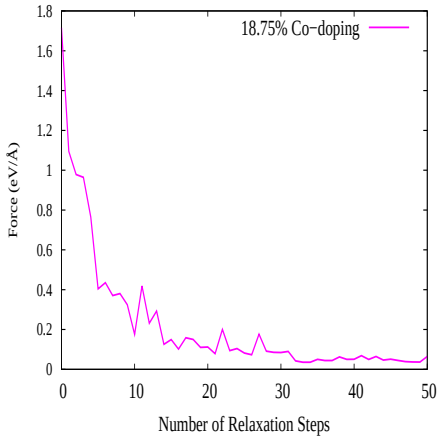

Fig. 2: Variation of Force Convergence with relaxation time steps

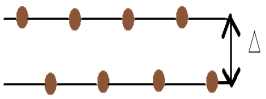

Fig. 3: Side view of Pristine Silicene with buckling $\Delta = 0.4350\ \AA$.

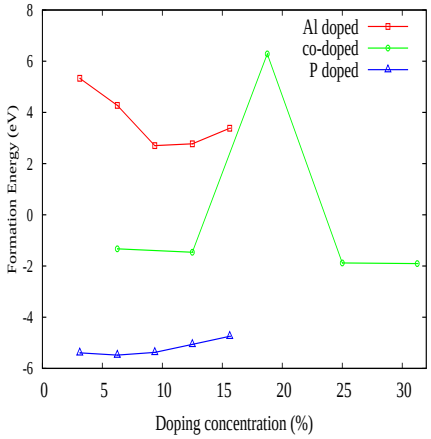

Fig. 4: Variation of formation energy with various doping concentrations

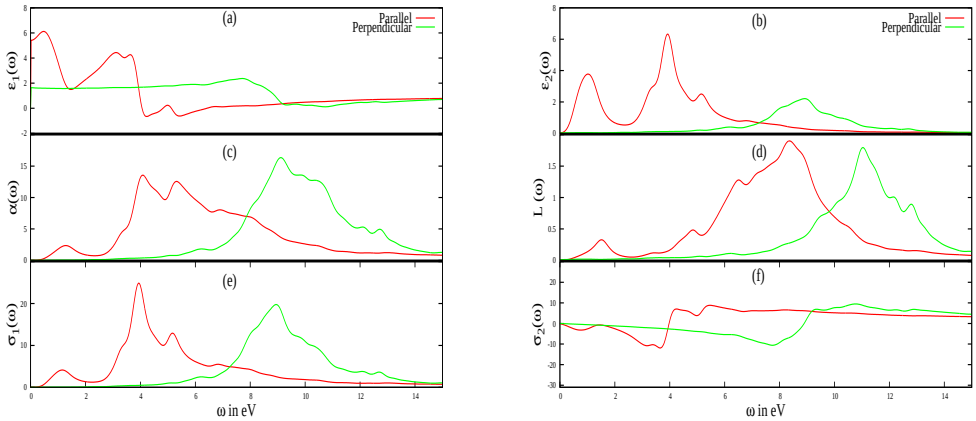

Fig. 5: Different frequency dependent optical properties of pristine silicene have been illustrated for both $E_{||}$ (red line) and $E_{\perp}$ (green line) of electric field vector. (a) Real part of $\varepsilon(\omega)$, (b) imaginary part of $\varepsilon(\omega)$, (c) absorption coefficient, (d) EELS function, (e) real part of $\sigma(\omega)$, (f) imaginary part of $\sigma(\omega)$

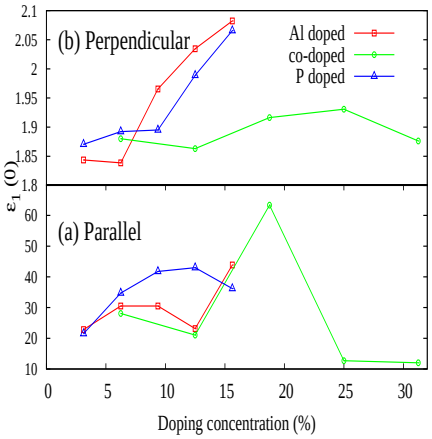

Fig. 6: Variation of static value of real part of the dielectric function ($\varepsilon_1(0)$) with various doping concentrations for $E_{||}$ and $E_{\perp}$.

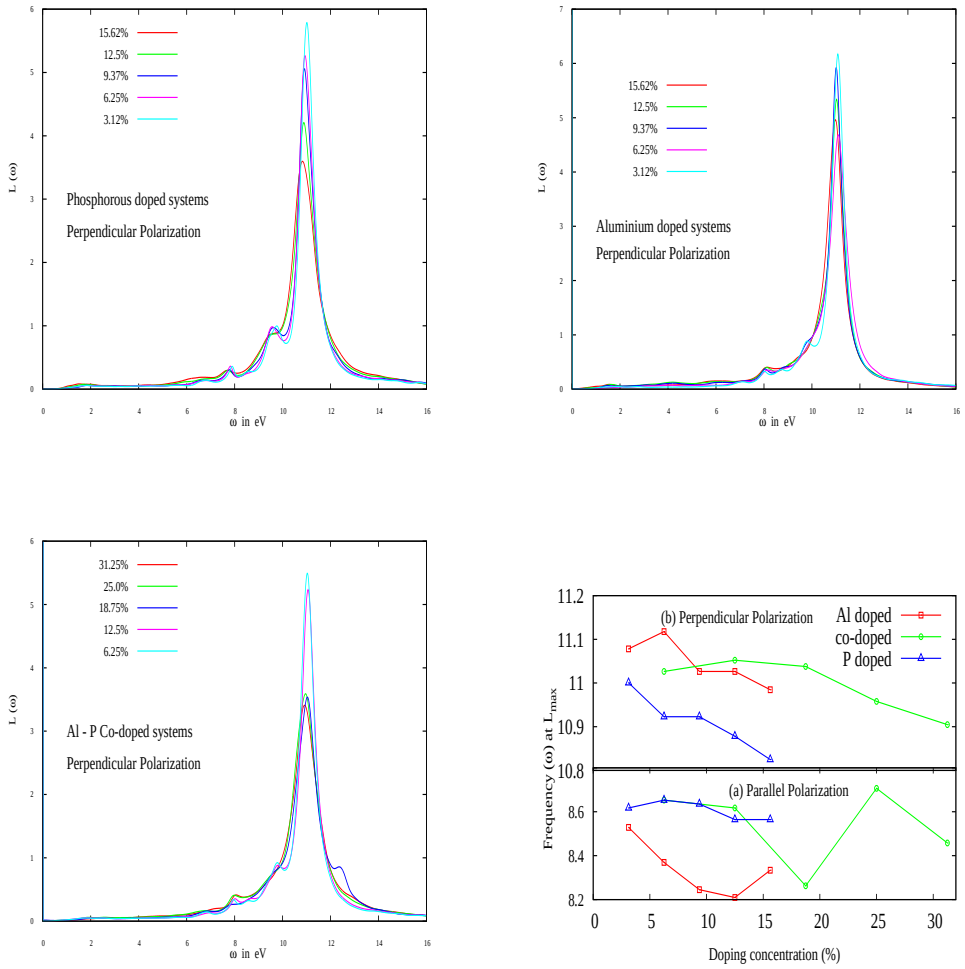

Fig. 7: (Top Panel) Depicts the EELS for some P doped system for $E_{\perp}$ (Left). (Top panel) Schematic Variation of EELS for Al doped system (Right). (Bottom Panel) Al-P Co-doped System (left). (Bottom Panel) Variation of frequencies (in eV) of the maximum values of EELS function with various doping concentration for $E_{||}$ and $E_{\perp}$ (Right)

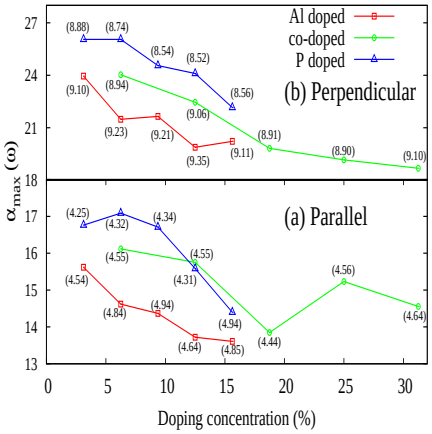

Fig. 8: Variation of maximum value of absorption coefficient ($\alpha(\omega)$) with various doping concentrations for $E_{||}$ and $E_{\perp}$ with frequency measured in eV

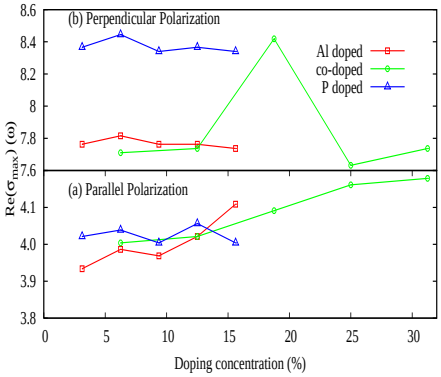

Fig. 9: Variation of maximum value of real part of the optical conductivity ($\sigma(\omega)$) with various doping concentrations for $E_{||}$ and $E_{\perp}$

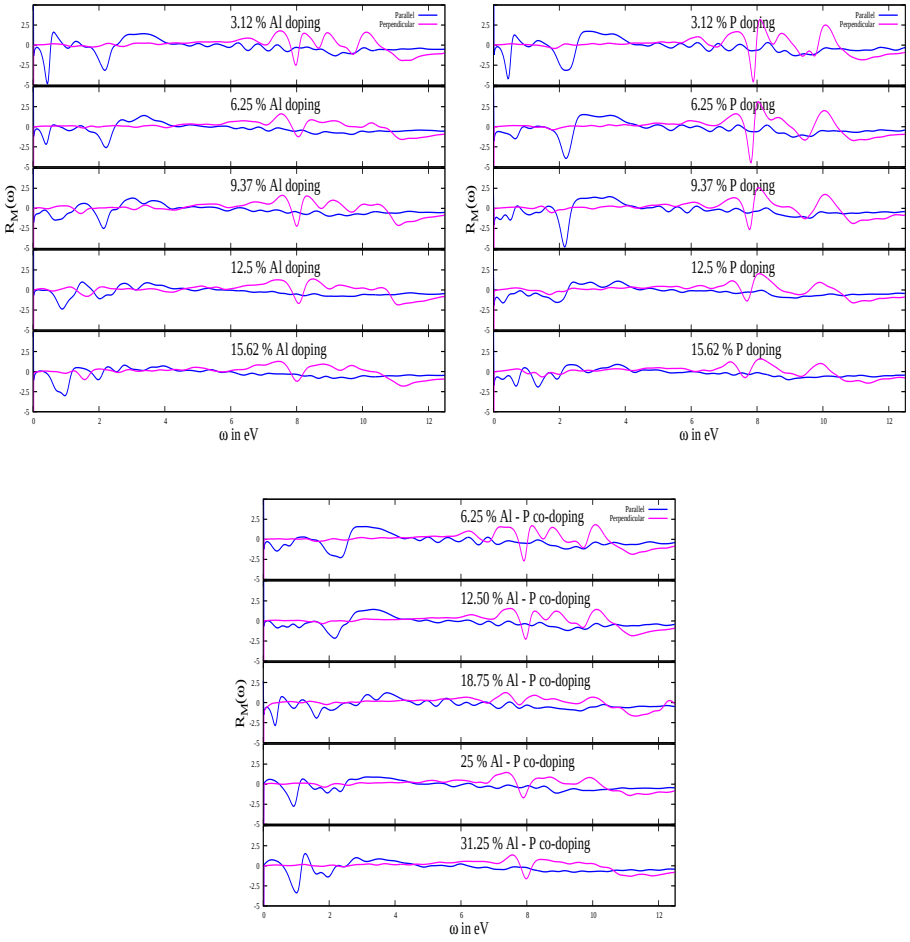

Fig. 10: The reflectivity modulation with energy for various doping concentrations of Al, P and Al-P co-doped for both type of polarizations.

Optical Properties of P and Al doped Silicene : A First Principles Study

Ritwika Das, Suman Chowdhury, Arnab Majumdar, Debnarayan Jana[1]

[1]Department of Physics, University of Calcutta, 92 Acharya Prafulla Chandra Road, Kolkata 700009, India

Summary

Various optical properties of two dimensional buckled silicene have been explored using spin unpolarized density functional theory by incorporating doping with phosporous and aluminium atoms in the hexagonal network of pristine buckled silicene.

Graphical Abstract